Exploring and Modeling Directional Effects on Steering Behavior in Virtual Reality

Yushi Wei ⓘ; Kemu Xu ⓘ, Yue Li ⓘ, Lingyun Yu ⓘ, and Hai-Ning Liang ⓘ, *Member, IEEE*

Abstract— Steering is a fundamental task in interactive Virtual Reality (VR) systems. Prior work has demonstrated that movement direction can significantly influence user behavior in the steering task, and different interactive environments (VEs) can lead to various behavioral patterns, such as tablets and PCs. However, its impact on VR environments remains unexplored. Given the widespread use of steering tasks in VEs, including menu adjustment and object manipulation, this work seeks to understand and model the directional effect with a focus on barehand interaction, which is typical in VEs. This paper presents the results of two studies. The first study was conducted to collect behavioral data with four categories: movement time, average movement speed, success rate, and reenter times. According to the results, we examined the effect of movement direction and built the $S\theta Model$. We then empirically evaluated the model through the data collected from the first study. The results proved that our proposed model achieved the best performance across all the metrics ($r^2 > 0.95$), with more than 15% improvement over the original Steering Law in terms of prediction accuracy. Next, we further validated the $S\theta Model$ by another study with the change of device and steering direction. Consistent with previous assessments, the model continues to exhibit optimal performance in both predicting movement time and speed. Finally, based on the results, we formulated design recommendations for steering tasks in VEs to enhance user experience and interaction efficiency.

Index Terms—Virtual reality; human performance modeling; steering law; barehand interaction; head-mounted display

◆

1 INTRODUCTION

Using mathematical models to generalize and encapsulate human behaviors within interactive processes is a foundational topic in human-computer interaction (HCI) [5, 52, 60]. One of the most well-tested, validated, and commonly used models is the Steering Law, which is designed to predict movement time (*MT*) in steering-based tasks, where users are required to navigate an object from its initial position to the endpoint along paths with different configurations, including variations in path width and length [1]. Specifically, steering is a frequently encountered task across various application scenarios in virtual environments (VEs), including object translation, interface manipulation, and vehicle navigation. Thus, the Steering Law has become an indispensable tool for understanding users' behavioral patterns within those tasks. For example, in 2D-based interactive environments such as tablets, laptops, and smartphones, a multitude of extended models based on the Steering Law have been further proposed. These models aim to investigate and encompass a broader range of factors influencing human behavior, i.e., path curvature [24, 38, 57], scale [2, 56], starting position [66], and devices latency [55].

With the growing complexity of application scenarios and tasks, such as interface manipulation and object dragging, there is an increasing recognition of the impact of movement direction. Previous research in 2D environments has demonstrated that different movement directions can significantly influence user behavior and performance [4, 65]. These studies attribute the directional effect to the engagement of various muscle groups and the constraints imposed by the skeletal structure

of the arm under different directions [4]. Compared to traditional 2D interactions, contemporary virtual reality (VR) systems provide users with enhanced interactive freedom. Instead of being confined to a small screen and limited interactions using a stylus or mouse, users can now engage with 3D space using their own bodies, a form of interaction now referred to as spatial interaction. This includes actions like reaching out and grasping by their hand, enabling multi-directional interactions within a volumetric space, resulting in larger bodily movement amplitudes and different behavioral patterns [44].

However, it is important to acknowledge the gap in understanding how movement direction affects user behavior in VEs. Previous findings and extended models considering the directional effect based on 2D scenarios cannot be directly applied to 3D environments [47]. This is due to the increased freedom of interaction in 3D via spatial interaction, leading to more intricate interaction mechanisms and necessitating greater coordination or constraints in users' joint and muscle movements [12]. Consequently, with the rising adoption of VR head-mounted displays (HMDs) and the distinct attributes of 3D VEs, it is necessary to formulate new models. These models should intricately account for the distinctive qualities of VEs and the impact of direction in steering tasks, aiming to describe and encapsulate user behavioral patterns comprehensively and precisely.

Therefore, in this work, we conducted two user studies to achieve a comprehensive understanding of user behavior mechanisms. Departing from the traditional VR interaction approach of raycasting, we opted for a more intuitive method [34], utilizing barehand as a way of interaction. This decision was guided by two primary considerations: (1) Barehand-based steering involves more extensive body movements, engages a broader range of muscles, and encompasses various poses [3, 40]. This increased physical activity provides a clearer view of the effects of different directions in steering tasks. (2) In 3D VR-based applications, barehand steering provides a broader range of application scenarios. This is especially pertinent as users in VEs are often required to perform actions such as dragging objects or translating user interfaces along specific paths [26, 36].

These two comprehensive user studies allowed us to gain insights into how steering direction influences user behavior in 3D VEs. Within the first study, we collected user behavior data to understand performance and behavior under various directions (see Sec. 4). Next, the data guiding the development of our model is termed the $S\theta$ model. We then verified and evaluated the predictability of this model. The empirical findings demonstrated that the $S\theta$ model exhibited robust predictability for movement time ($R^2 = 0.958$), surpassing the original

Steering Law across all metrics (see Sec. 5). Subsequently, we changed the conditions and settings in the second study, such as the movement direction and the equipment used, to further examine the reliability of our model. The outcomes suggest that the $S\theta$ model still demonstrated the best performance in all metrics in predicting the movement time and average movement speed (see Sec. 6). Finally, drawing from our insights into the influence of direction on user behavior, we formulated design recommendations for future VR steering tasks (see Sec. 8).

The primary contributions of our work include: **(1)** Results and interpretation of the behavioral characteristics of barehand-based steering tasks across different steering directions. Our study recorded various behavioral data, including movement time, average movement speed, success rates, and reentry frequency, across a range of path conditions. Additionally, we explored the effect of factors like path width, length, and direction on these behavioral outcomes. **(2)** An enhanced and novel Steering Law model was proposed for predicting movement time (MT) in 3D virtual environments, accounting for varying directions during barehand-based steering tasks. **(3)** An evaluation of the proposed model led to two recommendations for designing steering-based tasks for VR HMDs.

2 RELATED WORK

This section provides an overview of the two most commonly used models in the HCI community, namely Fitts' law and Steering Law, which are both employed to predict movement time (*MT*) within different tasks. It subsequently discusses previous models that aim to explain and encapsulate the directional effect on human behaviors. Finally, the section discussed bare-hand-based interaction, elucidating its characteristics, advantages, and limitations.

2.1 Modeling Pointing and Steering

Fitts' law, the most widely used human-behavior-based probabilistic model in the HCI community [27, 35, 39], is designed to assess and predict users' performance based on the metric of movement time (*MT*) in pointing selection tasks [15, 16]. The original model, i.e., simply Fitts' model, is formulated using the index of difficulty (*ID*) as follows:

$$MT = a + b \cdot ID,$$
$$ID = \log_2\left(\frac{2A}{W}\right). \tag{1}$$

MT refers to the time taken during the selection from the initial position to the select point at the target and is primarily influenced by the value of *ID*, which is a combination of two parameters (*W* and *A*). Where *W* represents the width of the target, *A* refers to the amplitude (distance) between the starting location and the target, and *a* and *b* are empirical values derived via regression.

Inspired by Fitts' law, Steering Law was subsequently proposed by Accot and Zhai [1]. They extended the model from pointing selection to a trajectory-based task, which allows the model to have the capabilities to predict and interpret human behavior in the process of steering. The model can be represented as:

$$MT = a + b \int_C \frac{ds}{W(s)} \tag{2}$$

Where *C* denotes the path that needs steering through. Here, *s* and $W(s)$ represent the infinitesimal length and width at *s* of the path, respectively. *a* and *b* remain empirical constants. Furthermore, if the path width remains constant, the model can be further simplified as follows:

$$MT = a + b\frac{A}{W} \tag{3}$$

It should be noted that the definitions of *W* and *A* are not identical to Fitts' law due to the transformation of the objective tasks (from pointing selection to steering). In Eq. (3), *W* and *A*, respectively, refer to the path width and the entire path length.

2.2 Modeling Directional Effects on Pointing and Steering Tasks

The directional effects on users' behaviors have been demonstrated by many studies within various interaction scenarios [6, 10, 14, 49, 53]. However, most of these works only focus on observing and reporting the effects without employing mathematical models to summarize and generalize the effects directly. Therefore, owing to the limited number of models that have considered the effect of movement direction, we have subsequently summarized several typical models to offer a comprehensive overview and understanding of the directional effect and modeling methods.

The first exploration of the directional effect in pointing tasks in a 3D environment was undertaken by Murata and Iwase using electromagnetic devices [37]. They investigated the directional effect by setting eight different azimuth angles from 0° to 315°, increasing at intervals of 45° under the spherical coordinate system. Their results indicated that users exhibited optimal performance during horizontal movements (0° and 180°), as measured by *MT*, while the worst performance was observed during vertical movements (90° and 270°). Furthermore, they revealed a sinusoidal relationship between *MT* and movement directions, which was expressed as follows:

$$MT = a + b \cdot \left(\log_2\left(\frac{A}{W} + 1\right) + c \cdot \sin\theta\right) \tag{4}$$

Where *A* and *W*, same as Fitts' law, represent the movement amplitude and target width. The movement direction θ serves as an additional variable controlled by a constant value of *c*. *a* and *b* remain constants that are determined by regression.

The aforementioned result, the sinusoidal relationship between *MT* and direction, was further confirmed by Cha and Myung [11] in 3D electrical sensors and conducting wires-based environments. Nevertheless, they extended Murata and Iwase's model to include the inclination angle θ_1 and also introduced the concept of the effective size/width, denoted by $W + F$, where *F* represented the finger pad size used when pointing at the target [21]. Coefficients including *a*, *b*, *c*, and *d* are empirically determined in the model. (see Eq. (5)).

$$MT = a + b \cdot \theta_1 + c \cdot \sin\theta + d \cdot \log_2\left(\frac{2A}{W + F}\right) \tag{5}$$

Furthermore, in 3D VR HMDs, Machuca and Stuerzlinger [4] assessed the stereo deficiencies in virtual hand pointing tasks. It is important to note that their study was not conducted in an immersive virtual environment but rather utilized large 3D displays. They further observed that users typically exhibit better performance during horizontal movements compared to movements directed away from or toward the user. Accordingly, they integrated the parameter of changes in target depths into Fitts' law, represented as *CTD*, into their proposed model, demonstrating that an increase in *CTD* led to prolonged *MT* (see Eq. (6)).

$$MT = a + b \cdot \log_2\left(\frac{A}{W} + 1\right) + c \cdot CTD \tag{6}$$

Meanwhile, in 2D touch pointing tasks, the impact of movement direction was also identified and modeled by extended Fitts' law. Zhang et al. [65] integrated the movement direction ω in the model. Additionally, they incorporated the concept of projection to calculate the final width and height for the square target. Their model can be expressed as:

$$MT = a + b\left(\log_2\left(\sqrt{\omega\left(\frac{A}{W}\right)^2 + (1-\omega)\left(\frac{A}{H}\right)^2} + 1\right)\right) \tag{7}$$

More specifically, the variable ω signifies $cos^2(\theta)$. After $cos^2(\theta)$ divided by the original width *W* and height *H*, the effective width and height values projected by direction θ can be calculated. Furthermore,

their model integrates the directional effect within the logarithmic term. Compared to the previously mentioned models that treat directional effect as an independent variable, this model demonstrates a more concise consideration of the target's shape.

Finally, in the context of steering-based tasks, the effects of direction have only been examined and modeled within one study, focusing on the scenario involving a mouse and 2D computer display [47]. They also observed the sinusoidal relationship between direction and MT, the same as Fitts' law. Interestingly, they found that all the linear regression lines, generated by each $\frac{A}{W}$ values and MT, seem to converge to a single point. This implies a clear multiplicative relationship between movement time and $\frac{A}{W}$. Therefore, the relationship between Gradient and Intercept across all the directions can be regressed (Where a and b are empirical constants determined by regression):

$$\text{Intercept} = a + b \cdot (\text{Gradient}) \tag{8}$$

Moreover, the original equation for the Steering Law can be written as follows:

$$MT = \text{Intercept} + \frac{A}{W}(\text{Gradient}) \tag{9}$$

Combining Eq. (8) and Eq. (9), the Gradient can be expressed as:

$$\text{Gradient} = \frac{(MT + a)}{(A/W + b)} \tag{10}$$

Since the sinusoidal relationship between direction and MT was identified, the Gradient equation can also be formulated as:

$$\text{Gradient} = a + b \times sin\theta \tag{11}$$

Finally, substituting Eq. (10) into Eq. (11), the prediction model can be deduced [47]:

$$MT = a + \text{Gradient}\left(\frac{A}{W} + b\right) \tag{12}$$

2.3 Barehand Interactions in VR

With advancements in hand-tracking technology and its unique advantages in interactivity, users can now interact with the objects in a more natural and intuitive way without the need for additional equipment, such as controllers [41, 44, 45]. This has significantly enhanced the immersive experience, presence, and realism felt in virtual environments [9, 32, 51]. Nowadays, an increasing number of studies have focused on barehand-based interactions, exploring various scenarios, including objects or user interface manipulation [59, 61], target selection [11], text entry and selection [18, 54], and gaming [17, 42].

More relevant to our work are barehand-based steering interactions, which require users to make direct contact with objects, mirroring real-life scenarios; this is a common task in virtual environments where users arrange, drag, and translate objects to specific locations [46, 67]. However, there are still challenges that should be noted due to the features of barehand-based interaction.

Firstly, compared to the popular interaction method of raycasting, where an infinite-length ray is projected from the controller in the forward direction, using barehand usually requires more effort to interact with objects [48]. This increased effort is due to the need for more physical movement and mental attention to coordinate different body parts for interaction. For instance, grasping distant objects by the hand necessitates the simultaneous engagement of the hand, arm, and shoulder, often resulting in more extensive arm movements and complex body coordination than raycasting [12]. Accordingly, in steering-based tasks, using hands directly to steer toward the target can be more challenging and demanding for users; they must control the arm to directly steer the target while also maintaining the stability of various body parts to ensure precise path following [31, 40]. This challenge may directly result in users exhibiting different behavioral patterns, and

various factors such as path width, length, and direction may also have a different impact on user behavior than in previous works because of this challenge.

Secondly, another issue arises from finger occlusion when making contact with an object, commonly referred to as "Fat Finger" [7, 23]. For example, Lee and Zhai [30] conducted a study on users' pointing performance on a small 2D screen, revealing that the original Fitts' law loses accuracy when the button size is sufficiently small. Additionally, in a 2D pointing task, Ko et al. [28] proposed a model to mitigate the "Fat Finger" effect by adjusting the effective width and height of the target in their model to account for finger touch ambiguity based on FFitts' law [7]. However, there has been no study specifically examining the existence of finger occlusion effects in both 2D and 3D environments within steering tasks. It remains unclear whether finger contact ambiguity can directly affect users' steering performance when dealing with small objects during the task.

In summary, the impact of movement direction has been observed in various previous works, and several models have been proposed. However, it is noteworthy that only pointing selection tasks based on Fitts' law or 2D small-screen-based steering tasks have been conducted. Considering the discrepancies in interaction environments [25, 63] (2D versus 3D), degrees of interaction freedom [34, 50] (mouse versus barehand), and the objectives of tasks [22, 29] (pointing selection versus steering), there still exists a gap in knowledge and understanding regarding the directional effect in 3D immersive VR barehand-based steering tasks.

3 RESEARCH QUESTION

To facilitate future design references for corresponding tasks, a comprehensive understanding of the user behavior in the steering task across different directions in VEs is necessary. Therefore, we conducted this research to seek answers to the following questions (marked as **RQ#**):

RQ1. *Can various steering directions significantly impact user performance and behavior within immersive VEs?* As described in Sec. 2.2, previous work has demonstrated the factor of directions significantly affects user performance within various tasks in 2D-based interactive environments, such as tablet and PC [37, 47]. Nevertheless, the directional effects remain unexplored in the context of 3D interaction scenarios. Considering the disparities in interactivity between 2D and 3D, as described in Sec. 2.3, previous results cannot be directly applied to the VE based steering tasks. Therefore, it is necessary to examine the directional effects further when the interaction patterns and tasks undergo changes.

RQ2. *How do the path features influence user behavior in barehand steering tasks?* The effect of finger occlusion has been effectively demonstrated in different tasks where users interact with objects on a 2D screen using their fingers [7]. However, traditional steering tasks often utilize a mouse or a controller equipped with a small cursor to interact with the object, which allows users to conduct the steering tasks without occlusion or ambiguity [56, 58]. Thus, when the interactive methods transition to finger-direct touch-based interaction in VEs, it becomes essential to consider the potential impact caused by the characteristics of barehand and investigate whether the previously proposed effects of path characteristics, as described by the Steering Law, persist in this scenario.

RQ3. *If direction does indeed impact user steering performance, then is there a specific behavioral paradigm corresponding to different directions?* In previous studies on pointing selection or 2D-based steering tasks, researchers have identified a sinusoidal relationship between directions and movement time [47, 65]. This phenomenon is often attributed to the interplay between the structure of the arm's bones and the constraints of the muscles [4]. However, with the transition from 2D to 3D interaction environments, characterized by greater interaction freedom and increased demand for bodily movement, it remains uncertain whether steering behaviors in 3D barehand-based scenarios exhibit consistent patterns akin to the sinusoidal relationships observed in previous research.

RQ4. *If indeed different features of the path impact behavior, could it be feasible to model the representation of these effects mathemati-*

cally? In previous research, both Fitts' Law and the Steering Law have proposed numerous extended models tailored for different application scenarios, as discussed in Sec. 2. Therefore, we expect to explore whether, if RQ1-RQ3 are confirmed in this study, it would be possible to establish corresponding refinement models, enhancing the Steering Law's predictive and behavioral explanatory capacity and fostering a more profound comprehension of user behaviors.

4 USER STUDY1: DATA COLLECTION

This study aims to attain comprehensive insights into user behaviors and performance in the bare-hand-based steering task. Therefore, We collected behavioral data across various categories, including movement time, speed, success rate, and reentry times, across diverse path configurations such as width, length, and directions.

4.1 Methods

4.1.1 Participants and Apparatus

Twenty-four participants (12 men, 12 women) were recruited from a local university, representing diverse educational backgrounds (18 undergraduates, 2 master's, and 4 PhD students). The participants' ages ranged from 19 to 26, with a mean of 22.87 ($SD = 1.15$). Some participants self-reported having a certain degree of shortsightedness; therefore, we allowed them to wear glasses or contact lenses during the experiment, ensuring optimal visibility of the objects in the scene (that is, normal to corrected-to-normal eyesight). On average, participants self-rated their familiarity with VR systems as 4.81 ($SD = 1.63$) on a 7-point Likert scale, where higher scores indicate greater familiarity.

The study employed the Quest Pro, which is equipped with a resolution of 1800×1920 per eye, along with a horizontal field of view (FoV) of $106°$ and a vertical FoV of $95.57°$. The default refresh rate, 90Hz, was consistently applied throughout the process. The experimental program was developed using C# in Unity3D (version 2022.3.01f) alongside the SteamVR PlugIn (version 2.2.0). The program was deployed on a Windows 11 PC featuring an Intel Core i9 processor and an NVIDIA RTX 3090 graphics card. A three-meter USB-C cable facilitated the connection between the headset and the PC.

4.1.2 Stimuli and Task

The study determined all the stimuli through a pilot study to ensure optimal suitability. Specifically, 12 semi-transparent paths, each representing a distinct direction of movement, were situated 300 mm in front of the participants' headset [53]. Concurrently, a sphere, referred to as the target ball, was affixed at the starting position of each path [33] (see Figure 1 LEFT). Upon the commencement of each trial, the designated path became opaque, accompanied by arrows indicating the direction of movement required. Participants were then instructed to pinch and steer the ball along the path from its initial position to the endpoint. During the steering process, they could receive visual feedback regarding the position of the target ball along the path, enabling them to adjust their strategy accordingly, i.e., the tradeoff between speed and accuracy [1]. Throughout the trials, participants were not allowed to reset the process and restart it again within a single trial once it had begun, regardless of their actual or perceived performance falling short of their expectations [55].

4.1.3 Design and Procedure

The user study followed a $2 \times 3 \times 12$ within-subjects design, incorporating 3 independent variables across a total of 72 distinct conditions: path length A (350 mm and 450 mm), path width W (40 mm, 60 mm and 80 mm) and steering direction θ ($0°$ to $330°$, with an increment step of $30°$).

The path length was defined as the distance from the starting position to the end. Meanwhile, the path width refers to the diameter of the target ball [33]. Additionally, The steering direction θ was determined as the angle between the positive direction of the horizontal x-axis and the steering path [53, 65] (see Fig. 1).

The study encompassed 6 blocks, comprising 6 combinations between A and W, arranged in a randomized order in the experiment. Within each block ($A \times W$) contained 12 θ values, the sequence of θ
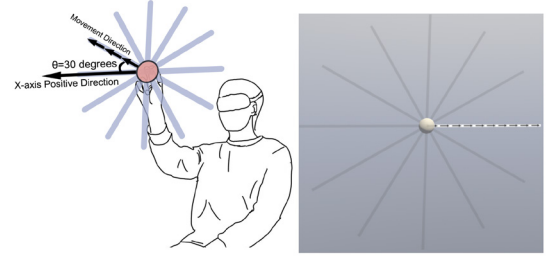

Fig. 1: A participant is steering the target ball (red sphere positioned at the center) along the designated path (indicated by arrows), where θ is defined as the angle formed between the direction of movement and the positive direction of the x-axis (directly to the right of where the participant is facing) (LEFT). A screenshot of the orthogonal first-angle view from the experimental program, where the positive direction of the x-axis coincides with the movement direction ($\theta = 0$) (RIGHT).

was also randomized, and participants were required to repeat 5 times in each condition (1 $A \times$ 1 $W \times$ 1 θ). Finally, a total of 8640 trials were collected from this study (2 $A \times$ 3 $W \times$ 12 θ $\times$ 5 repetitions $\times$ 24 participants)

Before the experiment, the participants were invited to complete a questionnaire to provide their demographic information. Following this, we introduced the VR headset and the task. They then wore the headset and adjusted it to a comfortable position under the guidance of a researcher. After the adjustment, participants commenced the practice trials, which lasted approximately three minutes until they felt familiar with the task and ready for the experiment. Subsequently, they proceeded to the formal trials. Throughout the task, participants were consistently instructed to prioritize both speed and accuracy while maintaining a seated position in an immobile and non-rotating chair.

The entire study lasted approximately 30 minutes for each participant. Considering the potential impact of fatigue caused by repetitive tasks [62] and the gorilla arm effect [20], which denotes users' tendency to experience fatigue when interacting with their arms in mid-air-based interactions, we allowed them to take breaks between each block, ensuring they were prepared before proceeding to the subsequent experiment.

4.1.4 Measurements

During the study process, our experimental program recorded four categories of data for each trial, i.e., movement time, average movement speed, success rate, and reentry times.

- **Movement Time (MT)**: The cumulative time throughout the entire steering process is one of the most commonly used metrics for evaluating users' behaviors and performance in steering tasks [1, 56].

- **Average Movement Speed (V)**: Determined by dividing the movement time by the path length, a higher speed indicates superior performance in the task [2, 19].

- **Success Rate**: Whether the user could steer the target ball without any interruption during the individual trial. This metric finally resulted in two states: success or failure.

- **Reentry Times**: The number of reentries between the finger and the target ball, reflecting the count of attempts made by participants to complete each trial. It may reveal the level of steering difficulty across various directions, with a higher count corresponding to more unsuccessful attempts and vice versa [4].

4.2 Results

Before data analysis, we employed two approaches to remove outliers. First, we excluded 214 trials, which accounted for 2.47% of the total number of trials, due to movement times exceeding 10 seconds. Subsequently, 114 (1.31%) trials were eliminated as they exceeded three times the standard deviations from the mean results regarding movement time or speed.
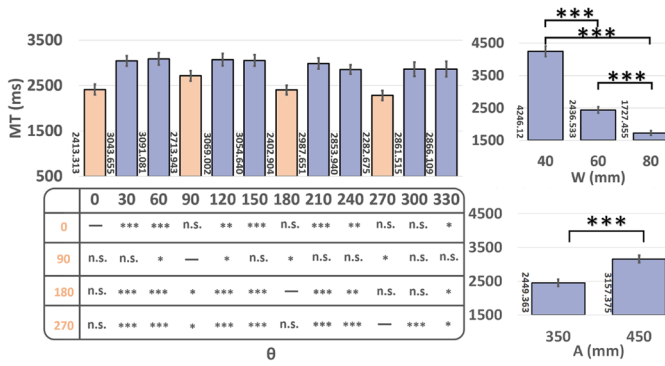
Fig. 2: Movement time (*MT*) for the variables that showed a significant main effect. The error bars show the standard error. The orange bars represent the quadrant boundary directions of the right ($\theta = 0$), the upward ($\theta = 90$), the left ($\theta = 180$), and the downward ($\theta = 270$). The table shows the p-values within each row indicating significant differences between quadrant boundary directions (number with orange at leftmost column) and others, with no significant differences observed between non-quadrant boundary directions. '***', '**', '*', and 'n.s.' indicate $p < 0.001$, $p < 0.01$, $p < 0.05$ and without statistical significance with a p-value less than 0.05.

In the following section, repeated-measures ANOVA (RM-ANOVA) tests were conducted to examine how the factors of path width, length, and direction affect movement time (Sec. 4.2.1), average movement speed (Sec. 4.2.2), success rate and reentry times (Sec. 4.2.3). We then provide our discussion and interpretation of the results (Sec. 4.3). Throughout the tests, the Greenhouse-Geisser was used to adjust the degrees of freedom if the assumption of sphericity was not met. Bonferroni corrections were used for post-hoc pairwise comparisons. All the repetitions were treated as an independent data point throughout the analysis process.

4.2.1 Movement Time

We found θ ($F_{11,253} = 15.359, p < 0.001, \eta_p^2 = 0.400$), A ($F_{1,23} = 128.517, p < 0.001, \eta_p^2 = 0.848$), and W ($F_{2,46} = 350.839, p < 0.001, \eta_p^2 = 0.938$) had significant main effects on movement time. when taking into account the interactions among these factors $\theta \times A$ ($F_{11,253} = 2.531, p = 0.005, \eta_p^2 = 0.099$), $\theta \times W$ ($F_{9.204,211.701} = 2.817, p = 0.004, \eta_p^2 = 0.109$) and $A \times W$ ($F_{1.999,45.987} = 17.289, p < 0.001, \eta_p^2 = 0.429$) also demonstrated a significant influence on movement time.

In relation to the factor θ, significant variations were noted among different conditions. Interestingly, these differences were only evident when comparing directions at quadrant boundaries ($0°, 90°, 180°, 270°$) to those not at quadrant boundaries or among quadrant boundary directions themselves. This suggests that no significant differences were observed among directions that were not at quadrant boundaries. Specifically, at 0 degrees, significant difference emerged when compared to 30 ($\Delta = -630.341$, $p < 0.001$), 60 ($\Delta = -677.768$, $p < 0.001$), 120 ($\Delta = -655.688$, $p = 0.001$), 150 ($\Delta = -641.327$, $p < 0.001$), 210 ($\Delta = -574.338$, $p < 0.001$), 240 ($\Delta = -440.627$, $p = 0.008$), and 330 ($\Delta = -452.796$, $p = 0.013$) degrees. At 90 degrees, meaningful distinctions surfaced in contrast to 60 ($\Delta = -377.138$, $p = 0.045$), 120 ($\Delta = -355.058$, $p = 0.047$), 180 ($\Delta = 311.039$, $p = 0.041$), and 270 ($\Delta = 431.268$, $p = 0.017$) degrees. At 180 degrees, substantial variations were evident in relation to 30 ($\Delta = -640.750$, $p < 0.001$), 60 ($\Delta = -688.177$, $p < 0.001$), 90 ($\Delta = -311.039$, $p = 0.041$), 120 ($\Delta = -666.097$, $p < 0.001$), 150 ($\Delta = -651.736$, $p < 0.001$), 210 ($\Delta = -584.747$, $p < 0.001$), 240 ($\Delta = -451.036$, $p = 0.001$), and 330 ($\Delta = -463.205$, $p = 0.049$) degrees. In terms of 270 degrees, the shortest time was observed among all directions, with pronounced disparities compared to 30 ($\Delta = -760.979$, $p < 0.001$), 60 ($\Delta = -808.406$, $p < 0.001$), 90 ($\Delta = -431.268$, $p = 0.017$), 120 ($\Delta = -786.326$,
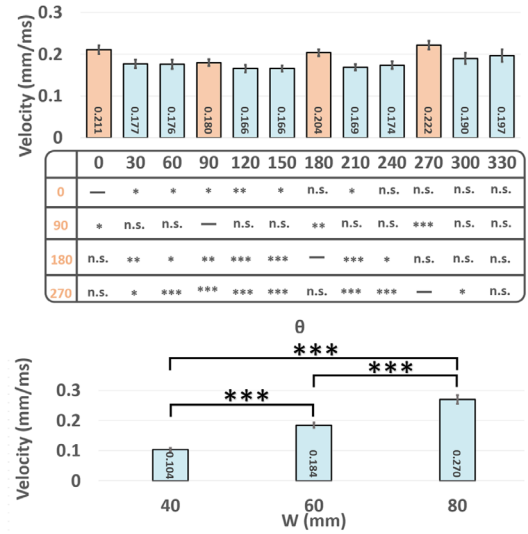

Fig. 3: Average movement speed (*V*) or the variables that showed a significant main effect. The error bars show the standard error. The orange bars represent the quadrant boundary directions of the right ($\theta = 0$), the upward ($\theta = 90$), the left ($\theta = 180$), and the downward ($\theta = 270$). The table shows the p-values within each row indicating significant differences between quadrant boundary directions (number with orange at leftmost column) and others, with no significant differences observed between non-quadrant boundary directions. '***', '*', and 'n.s.' indicate $p < 0.001$, $p < 0.05$ and without statistical significance with a p-value less than 0.05.

$p < 0.001$), 150 ($\Delta = -771.965$, $p < 0.001$), 210 ($\Delta = -704.976$, $p < 0.001$), 240 ($\Delta = -571.265$, $p < 0.001$), 300 ($\Delta = -578.840$, $p < 0.001$) and 330 ($\Delta = -583.433$, $p = 0.006$) degrees.

Concerning factor A, it can be observed that when A is 350 mm, the time spent is significantly less than 450 mm ($\Delta = -708.012$, $p < 0.001$). Additionally, when the value of W is set at 40 mm, the time expended is significantly higher compared to when it is set at 60 mm ($\Delta = 1809.587$, $p < 0.001$) and 80 mm ($\Delta = 2518.665$, $p < 0.001$). The same pattern is witnessed when comparing the values of 60 mm and 80 mm ($\Delta = 709.078$, $p < 0.001$). These results were visualized in Fig. 2.

4.2.2 Average Movement Speed

The significant effect had found at θ ($F_{11,253} = 9.745, p < 0.001, \eta_p^2 = 0.298$), W ($F_{2,46} = 215.445, p < 0.001, \eta_p^2 = 0.904$) and $\theta \times W$ ($F_{22,506} = 1.844, p = 0.011, \eta_p^2 = 0.074$).

Specifically, when examining pairwise comparisons, we observed a significant increase in average movement speed at a θ of 0 compared to 30 ($\Delta = .034$, $p = 0.027$), 60 ($\Delta = .035$, $p = 0.040$), 90 ($\Delta = 0.019$, $p = 0.019$), 120 ($\Delta = .045$, $p = 0.005$), 150 ($\Delta = .045$, $p = 0.003$), and 210 ($\Delta = .042$, $p = 0.023$) degrees. A contrary trend was noted at 90 degrees, where the average movement speed was significantly lower than that of 0 ($\Delta = -0.031$, $p = 0.019$), 180 ($\Delta = -0.024$, $p = 0.001$), and 270 ($\Delta = -0.042$, $p < 0.001$) degrees. Furthermore, an increasing trend was evident at 180 degrees when compared to 30 degrees ($\Delta = 0.028$, $p = 0.002$), as well as in comparison to 60 ($\Delta = 0.029$, $p = 0.020$), 90 ($\Delta = 0.024$, $p = 0.001$), 120 ($\Delta = 0.038$, $p < 0.001$), 150 ($\Delta = 0.038$, $p < 0.001$), 210 ($\Delta = 0.036$, $p < 0.001$), and 240 ($\Delta = 0.031$, $p = 0.015$) degrees. When the angle was set to 270, a similar trend to that observed at 0 and 180 occurred, in contrast to the observations made at 30 ($\Delta = 0.045$, $p = 0.005$), 60 ($\Delta = 0.046$, $p < 0.001$), 90 ($\Delta = 0.042$, $p < 0.001$), 120 ($\Delta = 0.056$, $p < 0.001$), 150 ($\Delta = 0.056$, $p < 0.001$), 210 ($\Delta = 0.053$, $p < 0.001$), 240 ($\Delta = 0.048$, $p < 0.001$), and 300 ($\Delta = 0.031$, $p = 0.049$) degrees.

In terms of factor W, average movement speed at 40 mm existed statistical significance by falling behind those at 60 mm ($\Delta = -0.080$,
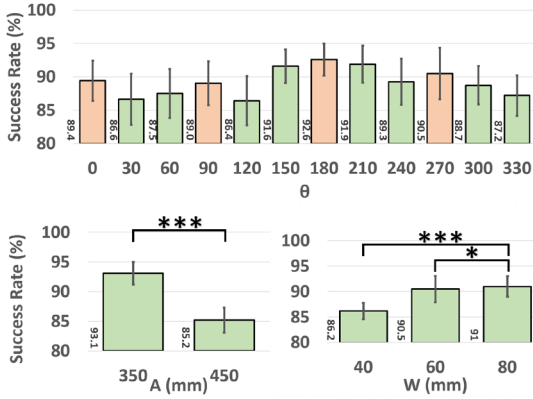
Fig. 4: Success rate for the variables that showed a significant main effect. The error bars show the standard error. '*' and '***' indicate $p < 0.05$ and $p < 0.001$, respectively. All effects demonstrated statistical significance with a p-value of at least less than 0.05. The orange bars represent the quadrant boundary of right ($\theta = 0$), the upward ($\theta = 90$), the left ($\theta = 180$), and the downward ($\theta = 270$).

Fig. 5: Reentry times for the variables that showed a significant main effect. The error bars show the standard error. '*', '**', and '***' indicates $p < 0.05$, $p < 0.01$ and $p < 0.001$, respectively. The orange bars represent the quadrant boundary of right ($\theta = 0$), the upward ($\theta = 90$), the left ($\theta = 180$), and the downward ($\theta = 270$).
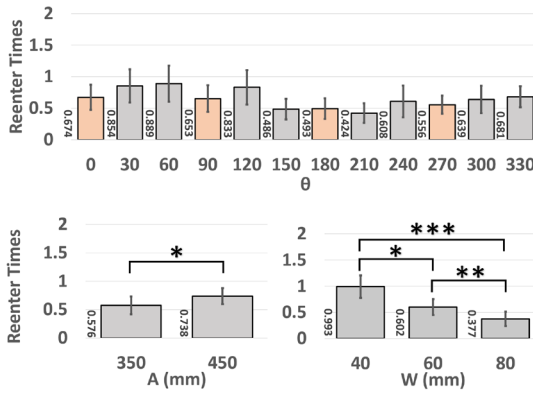
$p < 0.001$) and 80 mm ($\Delta = -0.166$, $p < 0.001$). The same trend was discovered between 60 mm and 80 mm ($\Delta = -0.085$, $p < 0.001$). The average movement speed results are shown in Fig. 3.

4.2.3 Success Rate and Reentry Times

Results of RM-ANOVAs showed that A ($F_{11,253} = 57.781, p < 0.001, \eta_p^2 < 0.715$) and W ($F_{2,46} = 8.646, p < 0.001, \eta_p^2 = 0.273$) had significant main effect on success rate. In the post-hoc pairwise comparison analysis of success rate, for the factor A, a notable improvement was noted when A was set at 350 mm as compared to 450 mm ($\Delta = 7.9\%$, $p = 0.025$) (see Fig. 4). Furthermore, in the factor of W, it was observed that larger values of W correlated with higher success rates. For instance, when W was 80 mm, the success rate was significantly higher compared to when it was 60 mm ($\Delta = 4.3\%$, $p = 0.029$) or 40 mm ($\Delta = 4.8\%$, $p < 0.001$).

In terms of reentry times, factor A ($F_{1,23} = 6.514, p = 0.018, \eta_p^2 = 0.221$) and W ($F_{2,46} = 3.118, p < 0.001, \eta_p^2 = 0.390$) demonstrates a significant main effect independently, while the interaction effect between A and W ($A \times W$) exhibits statistical significance ($F_{1.677,38.569} = 19.507, p < 0.001, \eta_p^2 = 0.459$). Following post-hoc pairwise comparisons, we observed that when A was set to 350 mm, the reentry times were significantly lower than when it was set to 450 mm ($\Delta = -0.162$, $p = 0.018$). Additionally, in terms of factor W, smaller values resulted

in higher reentry times. Specifically, when W was set to 40 mm, the number of repetitions was notably higher compared to when it was 60 mm ($\Delta = 0.391$, $p = 0.014$) or 80 mm ($\Delta = 0.616$, $p < 0.001$). This trend was also consistently demonstrated between 60 mm and 80 mm ($\Delta = 0.226$, $p = 0.001$) (see Fig. 5).

4.3 Discussion

4.3.1 Effects of Direction on Steering Performance in Immersive VEs (*RQ1*)

Statistical analysis (RM-ANOVA) revealed a significant influence of movement direction on user performance, particularly in movement time and average movement speed. However, this factor did not significantly affect success rate and reentry time. Specifically, the results of pos-hoc pairwise comparison analysis indicate that movement direction aligned with quadrant boundaries ($0°, 90°, 180°, 270°$) tend to perform better in terms of movement time compared to other directions (see Sec. 4.2.1). This trend is also reflected in the average movement speeds, where these directions consistently achieve higher speeds (see Sec. 4.2.2). Additionally, a similar pattern is observed in other metrics such as success rates and reentry times (see Sec. 4.2.3), which did not present a statistically significant effect, but still relatively suggesting smoother steering experiences with fewer interruptions. It can be inferred that participants have certain interaction strategies tailored to specific directions in steering tasks, effectively balancing efficiency and accuracy. For instance, they may fine-tune movement time and speed differently across various directions, with the goal of accomplishing tasks quickly while maintaining precision.

Moreover, our analysis revealed that among the four quadrant boundaries, the direction with the longest movement time is 90 degrees, while the shortest is 270 degrees ($P = 0.017$) (see Fig. 2). Similarly, this pattern is evident in average movement speed, indicating that the 90-degree direction is the slowest among the four quadrant boundaries, significantly slower than the speed in the 270-degree direction (the fastest) ($P < 0.001$) (see Fig. 3). However, regarding success rate and reentry time, although 270 degrees exhibited a higher success rate and fewer reentries compared to 90 degrees, there was no consistent trend suggesting that 90 degrees performed the worst while 270 degrees performed the best (see Fig. 5). Overall, a trend can be observed where efficiency tends to be higher in downward movements (from 30 to 150 degrees) than in upward movements in terms of movement time and average movement speed. This pattern could be attributed to inertia and gravitational forces acting on the hand during downward movement [8, 13]. Participants often relaxed their arms to control the descent rate, leading to faster speeds and shorter movement times.

Interestingly, our findings contrast with previous research, particularly in terms of movement time. Previous work, such as Murata et al. [37], suggested that vertical directions (90 and 270 degrees) tend to be less efficient than horizontal movements (0 and 180 degrees), which exhibit the lowest performance levels across all directions. Contrary to this, the findings of Study 1 demonstrated that horizontal movements did not show the best performance. Instead, the optimal performance was observed in downward movements (270 degrees), followed by horizontal (0 and 180 degrees) and upward movements (90 degrees). The Longer times and slower speeds were evident in movements along the diagonal directions. We attribute these contrary to to the ergonomic characteristics of the arm and hand structure, as well as the attentional demands inherent in barehand-based mid-air interactions across different directions, as supported by previous research [40, 43]. Specifically, diagonal movements require intricate coordination among the muscle groups responsible for shoulder, elbow, and wrist actions, a complexity surpassing that needed for vertical or horizontal movements [12]. Additionally, from a neurological perspective, executing diagonal movements is more demanding as it involves extensive processing of sensory data, including proprioceptive feedback and visual cues, to maintain precision and alignment with the intended path [48].

4.3.2 Effects of Path Characteristics on User Behavior (*RQ2*)

In line with the original Steering Law [1], we found that increased path length correlates with longer time spent, lower success rates, and higher

reentry times. Moreover, our empirical analysis results demonstrate a statistically significant main effect of path width on movement time, average movement speed, success rate, and reentry times.

Specifically, in terms of movement time, significant effects were observed regardless of path width and length (both $P < 0.001$). However, concerning average movement speed, only path width demonstrated a statistically significant impact on the outcome ($P < 0.001$) that was consistent with previous works [22]. Regarding success rate, both width and length exhibited similar performances (both $P < 0.001$). Nonetheless, it is worth noting that while width ($p < 0.001$) and length ($p = 0.018$) all demonstrated significant effects on reenter times, the impact of width appeared to be more pronounced. This phenomenon was further corroborated by pairwise comparisons among different widths, revealing significant differences between each condition. We attribute this phenomenon to the occlusion effect caused by the fingers. In our task design, users are required first to select the object (ball) and then steer it from the start position to the end. Therefore, the entire interaction process can be divided into two steps: pointing selection and steering. Initially, smaller objects may introduce more selection difficulty during the selection phase due to finger occlusion, as described in previous work [7]. Then, within the steering process, the fingers often obscure a significant portion of the ball, leading participants to struggle to discern whether they are properly gripping it. This causes them to deviate their fingers from the intended position easily. Thus, as the width of the ball increases, occlusion decreases, resulting in a notable reduction in reentry times.

5 MODELING AND FITTING

In the last section, we elucidated the directional effects on user behavioral patterns and steering task performance, including movement time, average movement speed, success rate, and reentry times. In light of the substantial effects observed, this section engages in a comprehensive analysis to encapsulate the effect through mathematical formulations (see Section 5.1). Subsequently, leveraging the formulated directional effects, we introduce an extended Steering Law model, termed the $S\theta$ Model (see 5.2). Finally, we evaluated the proposed model using the data collected from Study 1, confirming its capabilities in predicting movement time and explaining user behavior patterns (see 5.3.2).

5.1 Formulating the Effect of Direction

Section 4.2.1 presents results indicating a statistically significant relationship between θ and MT. The observed pattern illustrates that movement time reaches its minimum values when θ aligns with the quadrant boundary directions, which exhibits a strong periodicity, consistent with a sine function with a periodicity of $\frac{\pi}{2}$ (see Figure 6). Based on the observed pattern, we propose a new formula, which is a revision of the original sine function, name θ^{effect}, aims to depict the directional effects:

$$\theta^{effect} = a\sin\left(4\theta - \frac{\pi}{2}\right) + b \qquad (13)$$

Within the formula, the coefficients a and b are determined empirically based on regression results. The coefficient 4 signifies that the period of the wave is one-fourth of a standard sine function, indicating that the waveform repeats itself every $\frac{\pi}{2}$. The term $-\frac{\pi}{2}$ in the equation represents the phase offset, denoting the horizontal displacement of the waveform relative to the origin or the standard sine wave. In this context, it indicates that the waveform is shifted to the right by $-\frac{\pi}{2}$, implying that the starting point aligns with $\theta = 0$ and is currently at the lowest value within the period.

Based on the formula of θ^{effect}, we fitted the data obtained from study 1 (see Fig. 6). The coefficients are as follows: $a = 350.134$, $b = 2803.343$, and $R^2 = 0.808$. The amplitude $a = 350.134$ in the sine function indicates the waveform's vertical span, representing the distance between its peak and trough ($2a$). This value is attributed to the variance between the quadrant boundary directions and the cardinal directions, which is consistent with the data observed in our user study. Furthermore, the vertical displacement $b = 2803.343$ signifies a shift
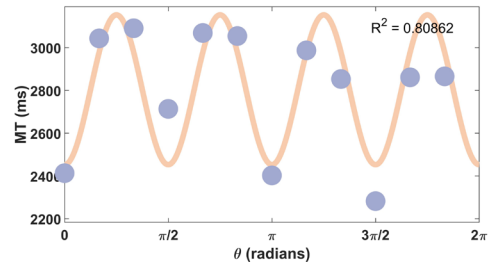
Fig. 6: The regression analysis showing the relationship between the variable θ (in radians), represented by purple circles, and the fitted regression curve (θ^{effect}), which is depicted in orange, on MT.

in the sine function graph relative to its original position by b units vertically. Notably, the positive value of b suggests an upward shift, aligning with the observed data.

In summary, the effect function demonstrated a robust fit and did not show any indications of overfitting, given its simple structure with only two interpretable coefficients. Moving forward, we integrated our effect function θ^{effect} into the original Steering Law, introducing an extended Steering Law model. This model is intended to precisely predicate behavioral patterns (MT), even when multiple movement directions are present and various path configurations are involved in the steering task.

5.2 Model Formulation

Before formulating the extended model, we examined the performance of the original Steering Law to assess its suitability for tasks involving diverse directions. Our empirical results showed that when we applied the conventional Steering Law to all 72 conditions (comprising $3W \times 2A \times 12D$), the fit was not as strong as expected, resulting in an R^2 value of only 0.850. However, when we tailored the Steering Law to each direction individually, we discovered that all 12 directions exhibited a robust fit, resulting in an outstanding average R^2 of 0.982 with a negligible standard deviation of 0.009.

Hence, we introduced a novel extended model in light of the suboptimal fitting results obtained and the observed θ^{effect}. In the modeling process, to maintain model simplicity and align with prior research [22, 37, 47], we treated θ as independent of both A and W. As a result, we separately incorporated θ into the existing Steering Law, culminating in the Steering Theta Model ($S\theta$ model):

$$\begin{aligned} S\theta Model = MT &= a + b\frac{A}{W} + c\theta^{effect} \\ &= a + b\frac{A}{W} + c\sin\left(4\theta - \frac{\pi}{2}\right) \end{aligned} \qquad (14)$$

Where a, b, and c are empirical values determined through regression.

5.3 Model Evaluation

5.3.1 Baseline Model and Comparison Metrics

To identify a model that effectively captures the characteristics of behavioral data while maintaining an appropriate level of simplicity, ensuring the credibility and utility of our results, we utilized three statistical metrics to evaluate and select the optimal model: the Akaike Information Criterion (AIC), the Bayesian Information Criterion (BIC), and the coefficient of determination (R^2). AIC and BIC balance model complexity and fit, preventing overfitting. AIC considers parameters and likelihood, while BIC adds a penalty for sample size. Lower AIC and BIC values indicate better performance of the model. R^2 measures how well the model explains variance in the dependent variable, with higher values indicating better fit.

5.3.2 Result of Evaluation

Tab. 1 lists the results of the linear regression. Two models, the conventional Steering Law and the $S\theta$ model, were tested. The results
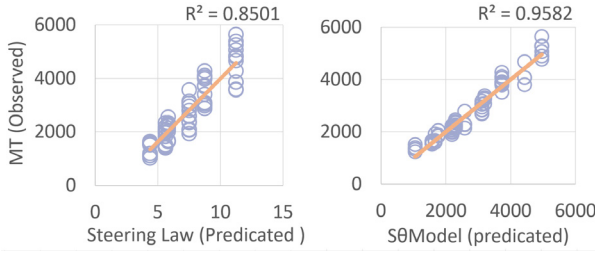
Fig. 7: Movement time (MT) model fitting across all conditions (N = 72) using the conventional Steering Law model and $S\theta$ model.

demonstrate that the $S\theta$ model performed best across all of the three metrics. Specifically, the $S\theta$ model exhibits outperformed fitness in R^2 than the baseline model ($\Delta = 0.13$). Both the AIC ($\Delta = -105.933$) and BIC ($\Delta = -103.663$) confirm that our model achieves a better balance between fit and simplicity compared to the baseline model. Additionally, in terms of the significant contributors of coefficients, both a and b are significant in both models, while c is also significant in the $S\theta$ model ($p < 0.001$).

5.4 Discussion

5.4.1 Formulation The Effect of Direction on Human Behavioral Pattern (*RQ3*)

Our results align with prior research, displaying significant periodicity (sine) on movement time. However, the period amplitude we observed is $\frac{\pi}{2}$, which deviates from the common periods of π or 2π reported in the literature [21,37,47,65]. In addition, since the minimum movement times consistently coincide with the quadrant boundary directions, we also shifted the sine function by $\frac{\pi}{2}$ radians to better align with the observed behavioral patterns. Finally, We formulated the θ^{effect} (refer to Eq. (13)) and successfully applied it to the dataset acquired from Study 1, attaining a substantial degree of fit ($R^2 = 0.808$) and confirming its strong interpretability of directional effects on behaviors.

5.4.2 Modeling User behavior in Steering Task (*RQ4*)

According to the sinusoidal relationship unveiled by θ^{effect}, we proposed the extended Steering Law model that incorporates the directional effects within the conventional model, termed the $S\theta$ model. We then evaluated the performance of our $S\theta$ model with three metrics (R^2, AIC, and BIC) and compared it to the Steering Law model (baseline).

The results indicated that in terms of fitness (R^2), the $S\theta$ model outperformed our baseline. As plotted in Fig. 7 LEFT, the baseline model lacked the capability to represent directional effects. Each value (determined by $\frac{A}{W}$) on the x-axis corresponds to twelve results where representing various directions from 0 to 330 degrees on the y-axis. Moreover, the trend of increased decentralization, caused by larger values of $\frac{A}{W}$ indicating greater difficulty, was observed. This tendency aligns with previous works suggesting that directional effects become more pronounced as the task difficulty increases [47,64]. In contrast to the baseline model, the $S\theta$ model exhibited well-fitted results (refer to Fig. 7 RIGHT), showcasing its strong predictive capability for steering tasks involving various movement directions. Furthermore, from the Tab. 1, both AIC and BIC suggest that $S\theta$ model exhibits superior performance in both fit quality and model complexity compared to the baseline. Briefly, despite the additional complexity introduced by the extra effect parameter in the $S\theta$ model, it substantially enhances data fit, thus outweighing the complexity penalty.

This conclusion is further supported by the parameter estimation, where the coefficient of θ^{effect} (c) demonstrated significant contributions to the final results in the $S\theta$ model ($p < 0.001$). Additionally, the 95% confidence interval (from 434.4 to 594.1) for parameter c excludes zero, further indicating a statistically significant relationship between θ and MT, implying its observed effect is not an incidental byproduct of random variations but rather a fundamental characteristic of the phenomenon under scrutiny.

5.4.3 Summary

Our empirical evidence confirmed that the θ^{effect} exhibits sinusoidal periodicity, but its period does not align with that observed in previous studies due to variations in task and interactive environments. Subsequently, we proposed the $S\theta$ model, which integrates the θ^{effect} into Steering Law. A thorough analysis revealed its superiority over the original Steering Law across all metrics and discussed the contributions for each coefficient, further confirming the importance and validity of incorporating the θ^{effect} into $S\theta$ model.

6 UTILITY OF THE PROPOSED MODEL

To further validate the applicability of our model, we conducted another user study using different devices to collect behavioral data within steering tasks involving different movement directions. We then applied the $S\theta$ model to predict movement time and average movement speed and validate the model's performance by comparing the predicted values with the collected data.

6.1 Participants and Apparatus

Twelve participants who had not participated in Study 1 were recruited from the local university in this study (6 males and 6 females; aged between 19 and 26, $M = 22.10$, $SD = 1.762$, 4 undergraduate students and 12 postgraduate students). Half of the participants have prior experience with VR HMDs. All of them reported they had normal or corrected-to-normal vision and were able to see all the objects clearly during the experiments. In terms of the device, we employed a different VR HMD compared to Study 1 to mitigate potential biases introduced by the experimental setting. Thus, we opted for the Meta Quest 3, which, although inferior in hardware performance compared to the Quest Pro, is more widely adopted by users. This device features a resolution of 2064×2208 per eye, a standard refresh rate of 90 Hz, and a FoV of 110 degrees horizontally and 96 degrees vertically.

7 TASK DESIGN AND PROCEDURE

We employed a within-subjects design with three factors: Path Length (A), Path Width (W), and Movement Directions (θ). Given our model incorporates θ^{effect} independently into the original Steering Law, variations in A and W do not affect the performance of our model. Therefore, the settings for A and W remained consistent with Study 1 to ensure simplicity and increased comparability. Regarding θ, as indicated by θ^{effect}, the longest movement time was expected to occur within the 45-degree interval (45, 135, 225, and 315 degrees) across all directions. Thus, to validate our observed results further, we adjusted the interval from 30 degrees in study 1 to 45 degrees.

The experimental procedure and condition order of these three factors were identical to those described in the first user study in 4.1.1. Therefore, a total of 2880 trials (12 participants $\times$ 2 A $\times$ 3 W $\times$ 8 θ $\times$ 5 repetitions) were collected after this study.

7.1 Predicting Movement Time

We pre-processed the outliers using the same method as in the first study. 79 trials (which accounts for 2.743% of the total data) were removed. Then, similar to Sec. 5, we employed the same approach and metrics to evaluate the performance of the baseline and our model.

As listed in Tab. 2, the $S\theta$ model exhibited the best performance across all metrics. The results empirically proved that the revision of θ values did not affect the performance of our model. In other words, irrespective of the movement direction, our model exhibits a robust capability to interpret user behavior patterns and predicate movement time across various orientations.

7.2 Predicting Movement Speed

Drawing from previous research [22], a linear correlation exists between movement time and average movement speed, expressed as $V = \frac{A}{MT}$. Hence, the formulation for average movement speed in the original Steering Law can be represented as $V = a + bW$. Accordingly,

Table 1: Models fitting results for predicting MT, including r^2 (where higher values indicate better fit), AIC, and BIC (where lower values indicate better performance). The empirical values a, b, and c are estimated regression coefficients with 95% CIs [lower, upper]. Significant contributors are indicated by '***' for p < 0.001. r^2, AIC and BIC in bold are the best values among them.

	Source	Model	a	b	c	r^2	AIC	BIC
Baseline	[1]	$a+b\frac{A}{W}$	-843.254*** [-1185.8, -500.7]	491.736*** [446.4, 536.9]		0.850	1082.465	1087.029
$S\theta$ model		$a+b\frac{A}{W}+c\theta^{effect}$	-842.143*** [-1029.5, -654.7]	491.773*** [466.9, 516.4]	514.353*** [434.4, 594.1]	**0.958**	**976.532**	**983.366**

Table 2: Models fitting results for predicting MT, including r^2 (higher values indicate better fit), AIC, and BIC (lower values indicate better performance). r^2, AIC, and BIC in bold are the best values among them.

	Model	r^2	AIC	BIC
MT	Original Steering Law	0.808	591.207	594.949
	$S\theta$ model	**0.910**	**521.242**	**526.856**
V	Original Steering Law	0.748	-311.197	-307.417
	$S\theta$ model	**0.889**	**-377.504**	**-371.890**

the $S\theta$ model can be reformulated as:

$$V = \frac{A}{a+b\frac{A}{W}+c\sin\left(4\theta-\frac{\pi}{2}\right)} \tag{15}$$

These two models were employed to scrutinize further and validate our proposed model's efficacy. Consistent with the results presented in Sec. 7.1, regarding average movement speed prediction, the $S\theta$ model consistently outperformed the baseline across all metrics.

8 SUMMARY OF FINDINGS AND RECOMMENDATIONS

Through the first user study, we collected the user behavioral data to gather a better understanding of how different factors, including path width, length, and directions, can affect user performance and behavior patterns in the steering task. The empirical data confirmed a significant relationship between path characteristics and four key metrics: movement time, average movement speed, success rate, and reentry times, where the effects of θ that aligned with quadrant boundary directions (0, 90, 180, and 270 degrees) exhibited significantly shorter time duration and faster speeds (see Sec. 3 RQ1). Moreover, our findings demonstrated that in 3D VR interactions, small targets could result in decreased interaction precision and accuracy due to the finger occlusion effect, mirroring challenges observed in 2D environments. We further identified the consistency of observed trends in terms of A and W with previous works to ensure the feasibility of modeling user performance through extending the original Steering Law that incorporated the effect of θ within barehand steering tasks (see Sec. 3 RQ2).

According to the results from the first user study, we formulated the effect of θ (θ^{effect}), which demonstrates a sinusoidal pattern accompanied by a unique periodicity ($\frac{\pi}{4}$) different from previous literature in varying contexts (see Sec. 3 RQ3). Next, an extended model ($S\theta$ model) was built by integrating the θ^{effect} into the conventional Steering Law. $S\theta$ model then achieved strong capabilities of accurately predicting movement time ($R^2 = 0.958$), representing a 10.8% improvement in R^2 and enhancements of 9.7% and 9.5% in AIC and BIC, respectively, compared to the conventional Steering Law (see Sec. 3 RQ4).

Moreover, we validated the utility of our proposed model through a user study involving revisions to devices and path features. The $S\theta$ model was used to predict movement time and average movement speed, which was derived by deforming the $S\theta$ model. The results demonstrated that, irrespective of path configuration and devices used, the $S\theta$ model always exhibited the highest predictive accuracy for both movement time and speed across all metrics.

Finally, based on the aforementioned findings, we propose two recommendations for 3D interface and interaction designers: Firstly, prioritize movement along quadrant boundary directions (0, 90, 180, and 270 degrees) when designing tasks or interactive techniques reliant on steering within virtual environments. This prioritization aims to enhance interaction efficiency and performance. Secondly, it is necessary to ensure that interactive elements, particularly in steering tasks, are adequately sized when designing for barehand-based interactions. They should be at least as large as the width of the user's interacting fingers. Neglecting this aspect could lead to finger occlusion effects, reducing interaction efficiency and leading users to repeat tasks multiple times, resulting in a suboptimal experience.

9 LIMITATIONS AND FUTURE WORK

We identified some limitations and possible avenues for future research. First, while our model has achieved promising results regarding typical steering tasks with only circular shape targets and constant straight paths in a controlled simplified background, we plan to extend our findings to real application scenarios with arbitrary target shapes, curved path characteristics, and complex backgrounds. Second, we employed a controlled distance between the user and the path in our user study design with fixed positions. While this approach was suitable for gathering behavioral data in a controlled user study environment, it may not fully represent real-world target steering scenarios. In many instances, users are required to steer targets using their hands at various distances and body positions, such as sitting, standing, or walking. It would be interesting to investigate whether behavioral patterns change under different hand movement depths and body positions during the steering process. Third, previous studies suggest inconsistent behavioral mechanisms may exist between people's dominant and non-dominant hands, as well as between left-handed and right-handed individuals during movement tasks. To better mirror real-world applications, all participants in our study were instructed to use their dominant hand. Additionally, randomizing our participant recruitment resulted in all participants being right-handed. This approach did not account for the behaviors associated with non-dominant hand usage and led to the underrepresentation of left-handed individuals in our participant pool. Consequently, this aspect might limit the optimal performance of our model in fully representing certain populations or application scenarios. Our planned future exploration will involve a wider sample population.

10 CONCLUSION

This work empirically investigated how direction and path characteristics (width and length) influence user behavior and performance in barehand-based steering tasks within 3D virtual environments. Leveraging the gathered behavioral data, we introduced an extended model of the Steering Law, termed the $S\theta$ model, specifically designed to predict movement time across various directions in steering tasks. Our evaluations validated the superior predictive capabilities of the proposed models compared to existing works. Additionally, to mitigate the risk of overfitting and further validate the model's applicability, we conducted a follow-up user study with adjusted values of movement directions and utilized different devices. The $S\theta$ model consistently outperformed the baseline across all metrics, reaffirming its efficacy. Overall, our findings contribute to a deeper understanding of user behavioral patterns in virtual environments, particularly regarding object manipulation or interface translation along designated paths.

REFERENCES

[1] J. Accot and S. Zhai. Beyond fitts' law: Models for trajectory-based hci tasks. In *Proceedings of the ACM SIGCHI Conference on Human Factors in Computing Systems*, CHI '97, p. 295–302. Association for Computing Machinery, New York, NY, USA, 1997. doi: 10.1145/258549.258760 1, 2, 4, 6, 9

[2] J. Accot and S. Zhai. Scale effects in steering law tasks. In *Proceedings of the SIGCHI Conference on Human Factors in Computing Systems*, CHI '01, p. 1–8. Association for Computing Machinery, New York, NY, USA, 2001. doi: 10.1145/365024.365027 1, 4

[3] A. Adkins, L. Lin, A. Normoyle, R. Canales, Y. Ye, and S. Jörg. Evaluating grasping visualizations and control modes in a vr game. 18(4), oct 2021. doi: 10.1145/3486582 1

[4] M. D. Barrera Machuca and W. Stuerzlinger. The effect of stereo display deficiencies on virtual hand pointing. CHI '19, p. 1–14. Association for Computing Machinery, New York, NY, USA, 2019. doi: 10.1145/3290605 .3300437 1, 2, 3, 4

[5] A. U. Batmaz, K. Yu, H.-N. Liang, and W. Stuerzlinger. Improving effective throughput performance using auditory feedback in virtual reality. In *Proceedings of the 2022 ACM Symposium on Spatial User Interaction*, SUI '22. Association for Computing Machinery, New York, NY, USA, 2022. doi: 10.1145/3565970.3567702 1

[6] H. Benko, A. D. Wilson, and P. Baudisch. Precise selection techniques for multi-touch screens. In *Proceedings of the SIGCHI Conference on Human Factors in Computing Systems*, CHI '06, p. 1263–1272. Association for Computing Machinery, New York, NY, USA, 2006. doi: 10.1145/1124772 .1124963 2

[7] X. Bi, Y. Li, and S. Zhai. Ffitts law: Modeling finger touch with fitts' law. In *Proceedings of the SIGCHI Conference on Human Factors in Computing Systems*, CHI '13, p. 1363–1372. Association for Computing Machinery, New York, NY, USA, 2013. doi: 10.1145/2470654.2466180 3, 7

[8] L. Bringoux, J. Lepecq, and F. Danion. Does visually induced self-motion affect grip force when holding an object? *Journal of neurophysiology*, 108 6:1685–94, 2012. doi: 10.1152/jn.00407.2012 6

[9] G. Buckingham. Hand tracking for immersive virtual reality: opportunities and challenges. *Frontiers in Virtual Reality*, 2:728461, 2021. 3

[10] S. K. Card, W. K. English, and B. J. Burr. Evaluation of mouse, rate-controlled isometric joystick, step keys, and text keys for text selection on a crt. *Ergonomics*, 21(8):601–613, 1978. 2

[11] Y. Cha and R. Myung. Extended fitts' law for 3d pointing tasks using 3d target arrangements. *International Journal of Industrial Ergonomics*, 43(4):350–355, 2013. 2, 3

[12] H. Chen, F. Qin, and J. Wu. Muscle synergy analysis on upper limb movements of human arms. In *Proceedings of the 2019 6th International Conference on Biomedical and Bioinformatics Engineering*, pp. 182–187, 2019. 1, 3, 6

[13] F. Crevecoeur, J. McIntyre, J. Thonnard, and P. Lefèvre. Gravity-dependent estimates of object mass underlie the generation of motor commands for horizontal limb movements. *Journal of neurophysiology*, 112 2:384–92, 2014. doi: 10.1152/jn.00061.2014 6

[14] A. Esenther and K. Ryall. Fluid dtmouse: Better mouse support for touch-based interactions. In *Proceedings of the Working Conference on Advanced Visual Interfaces*, AVI '06, p. 112–115. Association for Computing Machinery, New York, NY, USA, 2006. doi: 10.1145/1133265 .1133289 2

[15] P. M. Fitts. The information capacity of the human motor system in controlling the amplitude of movement. *Journal of experimental psychology*, 47(6):381, 1954. 2

[16] P. M. Fitts and J. R. Peterson. Information capacity of discrete motor responses. *Journal of experimental psychology*, 67(2):103, 1964. 2

[17] A. Georgiadis. Vr gaming-hands on: The use and effects of bare hand gestures as an interaction method in multiplayer virtual reality games, 2017. 3

[18] J. Grubert, L. Witzani, E. Ofek, M. Pahud, M. Kranz, and P. O. Kristensson. Text entry in immersive head-mounted display-based virtual reality using standard keyboards. In *2018 IEEE Conference on Virtual Reality and 3D User Interfaces (VR)*, pp. 159–166, 2018. doi: 10.1109/VR.2018.8446059 3

[19] T. Hidaka, Y. Sei, N. Nishida, S. Yamanaka, and B. Shizuki. Advanced investigation of steering performance with error-accepting delays. *International Journal of Human–Computer Interaction*, 0(0):1–14, 2023. doi:

[20] J. D. Hincapié-Ramos, X. Guo, P. Moghadasian, and P. Irani. Consumed endurance: A metric to quantify arm fatigue of mid-air interactions. In *Proceedings of the SIGCHI Conference on Human Factors in Computing Systems*, CHI '14, p. 1063–1072. Association for Computing Machinery, New York, NY, USA, 2014. doi: 10.1145/2556288.2557130 4

[21] E. R. Hoffmann. Effective target tolerance in an inverted fitts task. *Ergonomics*, 38(4):828–836, 1995. 2, 8

[22] E. R. Hoffmann. Review of models for restricted-path movements. *International Journal of Industrial Ergonomics*, 39(4):578–589, 2009. 3, 7, 8

[23] C. Holz and P. Baudisch. Understanding touch. In *Proceedings of the SIGCHI Conference on Human Factors in Computing Systems*, CHI '11, p. 2501–2510. Association for Computing Machinery, New York, NY, USA, 2011. doi: 10.1145/1978942.1979308 3

[24] X. Hu, X. Yan, Y. Wei, W. Xu, Y. Li, Y. Liu, and H.-N. Liang. Exploring the effects of spatial constraints and curvature for 3d piloting in virtual environments. In *Proceedings of the 23rd IEEE International Symposium on Mixed and Augmented Reality (ISMAR)*. IEEE, Hilton Bellevue, Greater Seattle Area, USA, October 21-25 2024. 1

[25] H. J. Jang, J. Y. Lee, J. Kwak, D. Lee, J.-H. Park, B. Lee, and Y. Y. Noh. Progress of display performances: Ar, vr, qled, oled, and tft. *Journal of Information Display*, 20(1):1–8, 2019. 3

[26] J. Kangas, S. K. Kumar, H. Mehtonen, J. Järnstedt, and R. Raisamo. Trade-off between task accuracy, task completion time and naturalness for direct object manipulation in virtual reality. *Multimodal Technologies and Interaction*, 6(1), 2022. doi: 10.3390/mti6010006 1

[27] R. Kerr. Movement time in an underwater environment. *Journal of Motor Behavior*, 5(3):175–178, 1973. 2

[28] Y.-J. Ko, H. Zhao, Y. Kim, I. Ramakrishnan, S. Zhai, and X. Bi. Modeling two dimensional touch pointing. In *Proceedings of the 33rd Annual ACM Symposium on User Interface Software and Technology*, UIST '20, p. 858–868. Association for Computing Machinery, New York, NY, USA, 2020. doi: 10.1145/3379337.3415871 3

[29] G. D. Langolf, D. B. Chaffin, and J. A. Foulke. An investigation of fitts' law using a wide range of movement amplitudes. *Journal of Motor Behavior*, 8(2):113–128, 1976. 3

[30] S. Lee and S. Zhai. The performance of touch screen soft buttons. In *Proceedings of the SIGCHI Conference on Human Factors in Computing Systems*, CHI '09, p. 309–318. Association for Computing Machinery, New York, NY, USA, 2009. doi: 10.1145/1518701.1518750 3

[31] O. Levin, M. Ouamer, M. Steyvers, and S. P. Swinnen. Directional tuning effects during cyclical two-joint arm movements in the horizontal plane. *Experimental Brain Research*, 141:471–484, 2001. 3

[32] L. Lin, A. Normoyle, A. Adkins, Y. Sun, A. Robb, Y. Ye, M. Di Luca, and S. Jörg. The effect of hand size and interaction modality on the virtual hand illusion. In *2019 IEEE Conference on Virtual Reality and 3D User Interfaces (VR)*, pp. 510–518, 2019. doi: 10.1109/VR.2019.8797787 3

[33] L. Liu, J.-B. Martens, and R. van Liere. Revisiting path steering for 3d manipulation tasks. In *2010 IEEE Symposium on 3D User Interfaces (3DUI)*, pp. 39–46, 2010. doi: 10.1109/3DUI.2010.5444724 4

[34] T. Luong, Y. F. Cheng, M. Möbus, A. Fender, and C. Holz. Controllers or bare hands? a controlled evaluation of input techniques on interaction performance and exertion in virtual reality. *IEEE Transactions on Visualization and Computer Graphics*, 2023. 1, 3

[35] I. S. MacKenzie. Fitts' law as a research and design tool in human-computer interaction. *Human-computer interaction*, 7(1):91–139, 1992. 2

[36] A. Masurovsky, P. Chojecki, D. Runde, M. Lafci, D. Przewozny, and M. Gaebler. Controller-free hand tracking for grab-and-place tasks in immersive virtual reality: Design elements and their empirical study. *Multimodal Technologies and Interaction*, 4(4), 2020. doi: 10.3390/mti4040091 1

[37] A. Murata and H. Iwase. Extending fitts' law to a three-dimensional pointing task. *Human movement science*, 20(6):791–805, 2001. 2, 3, 6, 7, 8

[38] M. Nancel and E. Lank. Modeling user performance on curved constrained paths. In *Proceedings of the 2017 CHI Conference on Human Factors in Computing Systems*, CHI '17, p. 244–254. Association for Computing Machinery, New York, NY, USA, 2017. doi: 10.1145/3025453.3025951 1

[39] A. Oulasvirta, P. O. Kristensson, X. Bi, and A. Howes. *Computational interaction*. Oxford University Press, 2018. 2

[40] C. Papaxanthis, T. Pozzo, and P. Stapley. Effects of movement direction

upon kinematic characteristics of vertical arm pointing movements in man. *Neuroscience Letters*, 253(2):103–106, 1998. 1, 3, 6

[41] S. Pei, A. Chen, J. Lee, and Y. Zhang. Hand interfaces: Using hands to imitate objects in ar/vr for expressive interactions. In *Proceedings of the 2022 CHI Conference on Human Factors in Computing Systems*, CHI '22. Association for Computing Machinery, New York, NY, USA, 2022. doi: 10.1145/3491102.3501898 3

[42] A. Renaux, F. Muhla, F. Clanché, P. Meyer, S. Maïaux, S. Colnat-Coulbois, and G. Gauchard. Effects of using immersive virtual reality on time and steps during a locomotor task in young adults. *Plos one*, 17(10):e0275876, 2022. 3

[43] R. L. Sainburg and D. Kalakanis. Differences in control of limb dynamics during dominant and nondominant arm reaching. *Journal of neurophysiology*, 83(5):2661–2675, 2000. 6

[44] R. Shi, Y. Wei, X. Qin, P. Hui, and H.-N. Liang. Exploring gaze-assisted and hand-based region selection in augmented reality. *Proc. ACM Hum.-Comput. Interact.*, 7(ETRA), may 2023. doi: 10.1145/3591129 1, 3

[45] R. Shi, J. Zhang, Y. Yue, L. Yu, and H.-N. Liang. Exploration of bare-hand mid-air pointing selection techniques for dense virtual reality environments. In *Extended Abstracts of the 2023 CHI Conference on Human Factors in Computing Systems*, CHI EA '23. Association for Computing Machinery, New York, NY, USA, 2023. doi: 10.1145/3544549.3585615 3

[46] G. E. Su, M. S. Sunar, and A. W. Ismail. Device-based manipulation technique with separated control structures for 3d object translation and rotation in handheld mobile ar. *International Journal of Human-Computer Studies*, 141:102433, 2020. 3

[47] N. Thibbotuwawa, R. S. Goonetilleke, and E. R. Hoffmann. Constrained path tracking at varying angles in a mouse tracking task. *Human Factors*, 54(1):138–150, 2012. 1, 3, 7, 8

[48] K. I. Ustinova, A. G. Feldman, and M. F. Levin. Central resetting of neuromuscular steady states may underlie rhythmical arm movements. *Journal of neurophysiology*, 96(3):1124–1134, 2006. 3, 6

[49] D. Vogel and P. Baudisch. Shift: A technique for operating pen-based interfaces using touch. In *Proceedings of the SIGCHI Conference on Human Factors in Computing Systems*, CHI '07, p. 657–666. Association for Computing Machinery, New York, NY, USA, 2007. doi: 10.1145/1240624.1240727 2

[50] C. Von Hardenberg and F. Bérard. Bare-hand human-computer interaction. In *Proceedings of the 2001 workshop on Perceptive user interfaces*, pp. 1–8, 2001. 3

[51] S. Vosinakis and P. Koutsabasis. Evaluation of visual feedback techniques for virtual grasping with bare hands using leap motion and oculus rift. *Virtual Reality*, 22(1):47–62, 2018. 3

[52] Y. Wei, R. Shi, D. Yu, Y. Wang, Y. Li, L. Yu, and H.-N. Liang. Predicting gaze-based target selection in augmented reality headsets based on eye and head endpoint distributions. In *Proceedings of the 2023 CHI Conference on Human Factors in Computing Systems*, CHI '23. Association for Computing Machinery, New York, NY, USA, 2023. doi: 10.1145/3544548.3581042 1

[53] T. G. Whisenand and H. H. Emurian. Analysis of cursor movements with a mouse. *Computers in Human Behavior*, 15(1):85–103, 1999. 2, 4

[54] W. Xu, X. Meng, K. Yu, S. Sarcar, and H.-N. Liang. Evaluation of text selection techniques in virtual reality head-mounted displays. In *2022 IEEE International Symposium on Mixed and Augmented Reality (ISMAR)*, pp. 131–140. IEEE, 2022. 3

[55] S. Yamanaka. Steering performance with error-accepting delays. In *Proceedings of the 2019 CHI Conference on Human Factors in Computing Systems*, CHI '19, p. 1–9. Association for Computing Machinery, New York, NY, USA, 2019. doi: 10.1145/3290605.3300800 1, 4

[56] S. Yamanaka and H. Miyashita. Scale effects in the steering time difference between narrowing and widening linear tunnels. In *Proceedings of the 9th Nordic Conference on Human-Computer Interaction*, NordiCHI '16. Association for Computing Machinery, New York, NY, USA, 2016. doi: 10.1145/2971485.2971486 1, 3, 4

[57] S. Yamanaka and H. Miyashita. Modeling pen steering performance in a single constant-width curved path. In *Proceedings of the 2019 ACM International Conference on Interactive Surfaces and Spaces*, ISS '19, p. 65–76. Association for Computing Machinery, New York, NY, USA, 2019. doi: 10.1145/3343055.3359697 1

[58] S. Yamanaka, H. Usuba, H. Takahashi, and H. Miyashita. Predicting success rates in steering through linear and circular paths by the servo-gaussian model. *International Journal of Human–Computer Interaction*, pp. 1–19, 2023. 3

[59] D. Yu, W. Jiang, A. Irlitti, T. Dingler, E. Velloso, J. Goncalves, and V. Kostakos. Haptics in vr using origami-augmented drones. In *2022 IEEE International Symposium on Mixed and Augmented Reality Adjunct (ISMAR-Adjunct)*, pp. 905–906, 2022. doi: 10.1109/ISMAR-Adjunct57072.2022.00198 3

[60] D. Yu, B. V. Syiem, A. Irlitti, T. Dingler, E. Velloso, and J. Goncalves. Modeling temporal target selection: A perspective from its spatial correspondence. In *Proceedings of the 2023 CHI Conference on Human Factors in Computing Systems*, CHI '23. Association for Computing Machinery, New York, NY, USA, 2023. doi: 10.1145/3544548.3581011 1

[61] D. Yu, Q. Zhou, T. Dingler, E. Velloso, and J. Goncalves. Blending on-body and mid-air interaction in virtual reality. In *2022 IEEE International Symposium on Mixed and Augmented Reality (ISMAR)*, pp. 637–646, 2022. doi: 10.1109/ISMAR55827.2022.00081 3

[62] D. Yu, Q. Zhou, B. Tag, T. Dingler, E. Velloso, and J. Goncalves. Engaging participants during selection studies in virtual reality. In *2020 IEEE Conference on Virtual Reality and 3D User Interfaces (VR)*, pp. 500–509, 2020. doi: 10.1109/VR46266.2020.00071 4

[63] L. Yu, P. Svetachov, P. Isenberg, M. H. Everts, and T. Isenberg. Fi3d: Direct-touch interaction for the exploration of 3d scientific visualization spaces. *IEEE Transactions on Visualization and Computer Graphics*, 16(6):1613–1622, 2010. doi: 10.1109/TVCG.2010.157 3

[64] X. Zhang. Understanding the effects of movement direction on 2d touch pointing tasks. ISS '23. Association for Computing Machinery, New York, NY, USA, 2023. 8

[65] X. Zhang, H. Zha, and W. Feng. Extending fitts' law to account for the effects of movement direction on 2d pointing. In *Proceedings of the SIGCHI Conference on Human Factors in Computing Systems*, CHI '12, p. 3185–3194. Association for Computing Machinery, New York, NY, USA, 2012. doi: 10.1145/2207676.2208737 1, 2, 3, 4, 8

[66] X. Zhou, X. Ren, and Y. Hui. Effect of start position on human performance in steering tasks. In *2008 International Conference on Computer Science and Software Engineering*, vol. 2, pp. 1098–1101, 2008. doi: 10.1109/CSSE.2008.1310 1

[67] F. Zhu and T. Grossman. Bishare: Exploring bidirectional interactions between smartphones and head-mounted augmented reality. In *Proceedings of the 2020 CHI Conference on Human Factors in Computing Systems*, CHI '20, p. 1–14. Association for Computing Machinery, New York, NY, USA, 2020. doi: 10.1145/3313831.3376233 3